Dyes and Pigments 91 (2011) 13–19

Contents lists available at ScienceDirect

Dyes and Pigments

journal homepage: www.elsevier.com/locate/dyepig

Hydrazones containing electron-accepting and electron-donating moieties

D. Gudeika [a], R. Lygaitis [a], V. Mimaitė [a], J.V. Grazulevicius [a,*], V. Jankauskas [b], M. Lapkowski [c,d], P. Data [c,d]

[a] Department of Organic Technology, Kaunas University of Technology, Radvilenu pl. 19, LT-50254 Kaunas, Lithuania
[b] Department of Solid State Electronics, Vilnius University, Sauletekio aleja 9, LT10222 Vilnius, Lithuania
[c] Faculty of Chemistry, Silesian University of Technology, ul. M. Strzody 9, 44-100 Gliwice, Poland
[d] Centre of Polymer and Carbon Materials of the Polish Academy of Sciences, Sowinskiego 5, 44-100 Gliwice, Poland

ARTICLE INFO

Article history:
Received 3 November 2010
Received in revised form
2 February 2011
Accepted 3 February 2011
Available online 23 March 2011

Keywords:
Hydrazone
Electron-accepting
Electron-donating
Glass-forming
Ionization potential
Charge mobility

ABSTRACT

Hydrazones containing electron-accepting 1,8-naphthalimide species and electron-donating triphenylamino moieties were synthesized and characterized by nuclear magnetic resonance, infrared spectroscopy, and mass spectrometry. Thermal, optical, electrochemical and photophysical properties of the synthesized derivatives were investigated, their, optical and electrochemical band-gap energies and ionization potentials were established. The hydrazones exhibit initial mass loss temperatures in the range of 268–348 °C and can form glasses with glass transition temperatures in the range of 46–142 °C as established by differential scanning calorimetry. Room temperature time-of-flight hole mobilities in the solid solutions of the derivatives in the polymeric host bisphenol-Z polycarbonate (50%) exceeded 10^{-5} cm^2/V s at high applied electric fields.

1. Introduction

Bipolar molecular glasses are of interest for the application in optoelectronic devices such as organic light-emitting diodes. Recently materials showing bipolar charge transport properties have been reported by several groups [1–3]. To achieve a good balance of holes and electrons, both hole and electron-transporting functions should be incorporated into a single bipolar material [4,5]. One promising strategy is to develop bipolar molecules bearing both electron-donating and electron-accepting moieties [6–8]. Such molecules can be also of interest as unimolecular half-substractors for molecular processors [9].

In this paper, we report the synthesis and a systematic investigation of hydrazones containing both donor (triphenylamino) and acceptor (1,8-naphthalimide) moieties. We have chosen these moieties in the design and synthesis of the bipolar compounds for the following reasons. High electron-affinity of 1,8-naphthalimides determines the possibility of their use as electron-transporting media, and the imide nitrogen makes 1,8-naphthalimides easy to functionalize [10]. Naphthalimide derivatives also represent an attractive class of electron-deficient organic materials for OLED applications. They exhibit good photochemical stability and high luminescence quantum yields [11]. As a matter of fact, the molecules bearing triphenylamino moiety are widely investigated mainly as hole-transporting materials, and their properties are described in a number of papers and reviews [12–14]. Triphenylamine and its derivatives, with excellent solubility, good stability, and high photoluminescent efficiency, are extensively used in optoelectronic devices [15]. The electron-donating nature of the derivatives of triphenylamine is the basis of their good hole-transporting properties.

2. Experimental Section

2.1. Chemicals

4-Bromo-1,8-naphtalic anhydride, 1-iodoethane (Aldrich), 2-ethylhexylamine (TCI), diphenylamine (Reakhim), 4-Iodoanisole (Aldrich), hydrazine hydrate (Aldrich), and the required chemicals, i.e. magnesium carbonate (Aldrich), potassium hydroxide (Aldrich), were purchased as reagent grade chemicals and used as received. The solvents, i.e. toluene (Aldrich), chloroform (Penta), dimethylformamide (Lachema), dichloromethane (POCH), ethylacetate (Penta), *n*-Hexane (Penta), diethyl ether (Penta), 2-methoxy ethanol (Aldrich), methanol (Penta), were purified and dried using the standard procedures [16].

* Corresponding author. Tel.: +370 37 300193; fax: +370 37 300152.
E-mail address: Juozas.Grazulevicius@ktu.lt (J.V. Grazulevicius).

0143-7208/$ – see front matter © 2011 Elsevier Ltd. All rights reserved.
doi:10.1016/j.dyepig.2011.02.002

2.2. Instrumentation

Infrared (IR) spectra were recorded using Perkin Elmer Spectrum GX spectrometer. UV spectra were recorded with Hitachi U-3000 spectrometer. The optical band gap was calculated from absorption edge (λ_{onset}) by conversion of wavelength to the energy using equation: $E_G = hc/\lambda_{onset}$ [eV] where, h is Planck's constant, c is speed of light in vacuum, λ_{onset} is absorption edge.

Fluorescence (FL) spectra were recorded with an MPF-4 spectrometer. Nuclear magnetic resonance (^{1}H NMR and ^{13}C NMR) spectra were obtained using a Varrian Unity Inova (300 MHz). All the data are given as chemical shifts ind (ppm), multiplicity, integration downfield from $(CH_3)_4Si$. Mass (MS) spectra were obtained on a Waters ZQ (Waters, Milford, USA). Thermogravimetric analysis was carried out using a Mettler TGA/SDTA851e/LF/1100 apparatus. The measurements were performed under nitrogen flow (75 cm^3 min^{-1}) in a temperature range from −30 to 850 °C at a heating rate of 20 °C/min. Differential scanning calorimetry (DSC) was carried out with Q100 TA DSC, with heating/cooling rates of 10 °C/min.

Charge carrier mobility (μ_h) was measured by time-of-flight method [17,18]. The samples for the measurements were prepared by the earlier reported procedure [19]. The electron-transporting layers were cast from the solutions of the compounds synthesized or from solutions of the mixtures of these compounds with polymer host bisphenol-Z polycarbonate (PC-Z) at mass proportion 1:1 in THF. The substrates were polyester film with Al layer. After coating the samples were heated at 80 °C for 1 h. Charge drift mobility was measured in electrophotographic regime. Electric field was created by positive corona charging. The charge carriers were generated at the layer surface by illumination with pulses of nitrogen laser (pulse duration was 2 ns, wavelength 337 nm). The layer surface potential decrease as a result of pulse illumination was up to 1–5% of initial potential before illumination. The capacitance probe that was connected to the wide frequency band electrometer measured the rate of the surface potential decrease *dU/dt*. The transit time t_t was determined from the kink on the curve of the *dU/dt* transient in log–log scale. The electron drift mobility was calculated by the formula $\mu_h = d^2/U_0 t_t$, where *d* is the layer thickness, U_0 − the surface potential at the moment of illumination.

Ionization potentials (I_p) were established by electron photoemission technique in air. The samples were prepared by the earlier reported procedure [20]. They were obtained by casting tetrahydrofurane solutions of the materials on aluminium foil coated with the adhesive layer of methylmetacrylate and metacrylic acid copolymer. The samples before measurements were dried at 80 °C in air for 1 h.

The solutions of the synthesized compounds compounds with the concentration of 1.0 mM were used for cyclic voltamperometry measurements. Electrochemical studies were conducted in 0.1 M solution of Bu_4NBF_4 (Sigma Aldrich 99%) in anhydrous dichloromethane at room temperature.

The electrochemical investigations were carried out using Eco Chemie Company's AUTOLAB potentiostat "PGSTAT20". The results were collected using GPES (General Purpose Electrochemical System) software. The electrochemical cell comprised platinum wire with 1 mm diameter of working area as working electrode, Ag wire − calibrated versus ferrocene/ferrocinium redox couple − as a quasi-reference electrode and platinum coil as auxiliary electrode. Cyclovoltammperometric measurements were conducted at 50 mV/s potential rate.

HOMO and LUMO energies were calculated by the following equations $E_{HOMO} = -(E_p + 4.8)$ [eV]; $E_{LUMO} = -(E_n + 4.8)$ [eV] where, E_n and E_p are the onsets of reduction and oxidation potentials versus the Fc/Fc$^+$. Electrochemical band gap was obtained from the equation: $E_G = E_{LUMO} - E_{HOMO}$ [eV].

2.3. Synthesis

2.3.1. 4-(Di(4-methoxyphenyl)amine)benzaldehyde (**a**) and 4,4′-diformyl-4″-methoxyphenylamine (**b**)

4-(Di(4-methoxyphenyl)amine)benzaldehyde (**a**) and 4,4′-diformyl-4″-methoxyphenylamine (**b**) were synthesized by the method of Vilsmeier [21].

2.3.2. 4-Bromo-N-(2-ethylhexyl)-1,8-naphthalimide (**1**)

Compound **1** was synthesized as described in the literature [22]. A solution of 4-bromo-1,8-naphtalic anhydride (1 g, 3.61 mmol) in 25 ml of dimethylformamyde (DMF) was added to a 100 ml three neck round bottom flask equipped with a reflux condenser and a magnetic stirrer. Then 2-ethylhexylamine (0.47 g, 3.61 mmol) was added drop-wise and the reaction mixture was heated up to 110 °C and stirred under nitrogen for 1.5 h. The end of the reaction was detected by TLC (eluent: toluene/ether, 6:1). The reaction mixture was concentrated using rotary evaporator and then the product was precipitated out into 1 N HCl, filtered off and washed with 1 N HCl. The crude product was purified by silica gel column chromatography using acetone and hexane mixture (vol. ratio 1:1.5) as an eluent. Yield: 0.86 g (62%) of yellow crystals. Mp = 82–83 °C ^{1}H NMR spectrum (300 MHz, CDCl3, δ, ppm): 8.70 (dd, 1H, $^5J_{HH}$ = 1.13 Hz, $^4J_{HH}$ = 7.31 Hz, 5-H$_{Naphthalene}$), 8.61 (dd, 1H, J_{HH} = 1.17 Hz, $^3J_{HH}$ = 8.56 Hz, 7-H$_{Naphthalene}$), 8.45 (d, 1H, $^4J_{HH}$ = 7.88 Hz, 3-H$_{Naphthalene}$), 8.08 (d, 1H, J_{HH} = 7.87 Hz, 2-H$_{Naphthalene}$), 7.89 (tr, 1H, J_{HH} = 7.32 Hz, J_{HH} = 8.52 Hz, 6-H$_{Naphthalene}$), 4.18–4.11 (m, 1H, −CH, 14-H$_{aliphatic}$), 1.60–1.34 (m, 10H, 5×CH$_2$, 13, 15, 16, 17, 19-H$_{aliphatic}$), 0.99–0.90 (m, 6H, 2×CH$_3$, 18, 20-H$_{aliphatic}$). IR, (in Br), cm^{-1}: 3070 ν (CH$_{ar}$); 2959, 2926, 2871, 2855 ν (CH$_{aliphatic}$); 1702 ν (C=O$_{anhydride}$); 1653, 1590, 1504, 1459 ν (C=C$_{ar}$); 1344, 1231 ν (C–N); 783 γ (CH$_{ar}$); 664, 563 ν (C–Br). ^{13}C NMR spectrum (300 MHz, CDCl3, δ, ppm): 164.26, 133.41, 132.32, 131.52, 131.35, 130.89, 130.38, 129.31, 128.34, 123.43, 122.57, 44.54, 38.17, 31.0, 28.95, 24.32, 23.32, 14.34, 10.90. MS (APCI$^+$, 20 V), *m/z*: 388 ([M + H]$^+$). Anal. Calcd. for $C_{20}H_{22}BrNO_2$: C, 61.86; H, 5.71; Br, 20.58; N, 3.61; O, 8.24. Found: C, 61.79; H, 5.75; Br, 20.62; N, 3.58; O, 8.21.

2.3.3. 4-Hydrazino-N-(2-ethylhexyl)-1,8-naphthalimide (**2**)

4-Bromo-*N*-(2-ethylhexyl)-1,8-naphthalimide (1.5 g, 3.86 mmol) and hydrazine hydrate (0.38 ml, 7.73 mmol) were dissolved in 40 ml of 2-methoxy ethanol and placed into an oven-dried, 150 ml two-necked round-bottomed flask equipped with a magnetic stir bar under an nitrogen atmosphere. The reaction mixture was refluxed at the room temperature for 1.5 h. The end of the reaction was detected by TLC (eluent: acetone/*n*-hexane, 1:1.5). The reaction mixture was concentrated using rotary evaporator and then the product was precipitated out into 1 N HCl, filtered off and washed with 1 N HCl. The crude product was purified by silica gel column chromatography using acetone and hexane mixture (vol. ratio 1:1.5) as an eluent. Yield: 0.67 g (52%) of yellow crystals. Mp = 81–82 °C ^{1}H NMR spectrum (300 MHz, CDCl3, δ, ppm): 8.64 (dd, 1H, J_{HH} = 1.01 Hz, J_{HH} = 7.31 Hz, 5-H$_{Naphthalene}$), 8.58 (d, 1H, J_{HH} = 8.36 Hz, 7-H$_{Naphthalene}$), 8.09 (d, 1H, $^4J_{HH}$ = 1.05 Hz, 3-H$_{Naphthalene}$), 8.06 (d, 1H, J_{HH} = 1.06 Hz, 2-H$_{Naphthalene}$), 7.69 (d, 1H, J_{HH} = 1.04 Hz, 6-H$_{Naphthalene}$), 6.61 (s, 1H, −NH), 4.15–4.12 (m, 1H, CH$_{aliphatic}$), 3.88 (s, 2H, −NH$_2$), 1.60–1.32 (m, 10H, 5×CH$_2$, 13, 15, 16, 17, 19-H$_{aliphatic}$), 1.01–0.87 (m, 6H, 2×CH$_3$, 18, 20-H$_{aliphatic}$). IR, (in Br), cm^{-1}: 3341, 3310 ν (NH$_2$); 3295 ν (NH); 3073 ν (CH$_{ar}$); 2950, 2924, 2868 ν (CH$_{aliphatic}$); 1693 ν (C=O$_{anhydride}$); 1642, 1616, 1581, 1543 ν (C=C$_{ar}$); 1392, 1358 ν (C–N); 778 γ (CH$_{ar}$); ^{13}C NMR spectrum (300 MHz, CDCl3, δ, ppm): 133.71, 133.12, 132.71, 132.15, 131.69, 131.30, 131.09, 130.96, 127.16, 125.19, 113.62, 54.13, 53.82, 47.32, 45.03, 32.68, 29.22, 27.91, 27.52. MS (APCI$^+$, 20 V), *m/z*: 339 ([M + H]$^+$). Anal. Calcd. for

$C_{20}H_{25}N_3O_2$: C, 70.77; H, 7.42; N, 12.38; O, 9.43. Found: C, 70.81; H, 7.39; N, 12.33; O, 9.48.

2.3.4. 4,4′-diformyl-4″-methoxyphenylamine bis(N-(2-ethylhexyl)-1,8-naphthalimide) hydrazone (**3**)

4,4′-Diformyl-4″-methoxyphenylamine (**b**) (0.1 g, 0.03 mmol) and 25 ml of methanol were placed into 250 ml 2-neck round bottom flask equipped with reflux condenser and mechanical stirrer and heated at 60 °C untill the homogeneous solution was obtained. Then the solution of 4-hydrazino-*N*-(2-ethylhexyl)-1,8-naphthalimide (0.026 g, 0.08 mmol) in 15 ml of methanol was added drop-wise. The mixture was refluxed until the dialdehyde (**b**) fully reacted (1.5 h, TLC control: eluent acetone/*n*-hexane 1:3). After the reaction, the mixture was slowly cooled to the room temperature. Crystals formed upon standing were filtered off, washed with methanol and dried to obtain 0.02 g (70%) of compound **3**. Mp = 158–159 °C ^{1}H NMR spectrum (300 MHz, CDCl3, δ, ppm): 8.80 (s, 2H, 2×N–CH), 8.61 (kv, 6H, J_{HH} = 7.70 Hz, J_{HH} = 17.57 Hz, $H_{Naphthalene}$), 8.25 (d, 2H, J_{HH} = 8.58 Hz, $H_{Naphthalene}$), 8.07 (d, 2H, J_{HH} = 4.21 Hz, $H_{Naphthalene}$), 7.81–7.59 (m, 10H, ar), 7.54 (kv, 2H, J_{HH} = 3.34 Hz, J_{HH} = 5.74 Hz, ar), 4.09 (p, 4H, J_{HH} = 6.59 Hz, J_{HH} = 13.41 Hz, 2×N–CH_2, aliphatic), 3.84 (s, 3H, –OCH_3), 3.49 (s, 2H, 2×NH), 1.44–1.32 (m, 16H, 8×CH_2, aliphatic), 0.98–0.85 (m, 12H, 4×CH_3, aliphatic). IR, (in Br), cm^{-1}: 3284 ν (NH); 3060 ν (CH_{ar}); 2954, 2926, 2856 ν ($CH_{aliphatic}$); 1691 ν (C=$O_{anhydride}$); 1651, 1614, 1578, 1504 ν (C=C_{ar}); 1460, 1427 γ (OCH_3); 1387, 1352 ν (C–N); 827, 774 γ (CH_{ar}); ^{13}C NMR spectrum (300 MHz, CDCl3, δ, ppm): 165.16, 164.73, 152.42, 151.31, 149.06, 145.40, 134.18, 131.62, 131.50, 131.42, 129.89, 128.86, 128.42, 125.82, 120.03, 118.97, 115.58, 115.40, 55.80, 44.31 38.22, 31.05, 29.02, 24.35, 23.36, 14.37, 10.95. MS (APCI$^+$, 20 V), *m*/*z*: 973 ([M + H]$^+$). Anal. Calcd. for $C_{16}H_{63}N_7O_5$: C, 75.21; H, 6.52; N, 10.06; O, 8.21. Found: C, 75.30; H, 6.56; N, 10.12; O, 8.23.

2.3.5. 4-(Di(4-methoxyphenyl)amine)benzaldehyde N-(2-ethylhexyl)-1,8-naphthalimide hydrazone (**4**)

Compound **4** was synthesized by the same procedure as compound **3**, only compound (**a**) was used instead of compound (**b**). The yield of red crystals 4 was 0.09 g (56%). Mp = 125–126 °C ^{1}H NMR spectrum (300 MHz, CDCl3, δ, ppm): 8.59 (d, 1H, J_{HH} = 7.71 Hz, $H_{Naphthalene}$), 8.53 (d, 1H, J_{HH} = 8.30 Hz, $H_{Naphthalene}$), 8.21 (d, 2H, J_{HH} = 8.40 Hz, $H_{Naphthalene}$), 7.74 (d, 1H, J_{HH} = 8.3 Hz, $H_{Naphthalene}$), 7.55 (d, 2H, J_{HH} = 8.74 Hz, ar), 7.18–7.09 (m, 4H, ar), 6.96–6.84 (m, 6H, ar), 4.12 (p, 2H, J_{HH} = 5.49 Hz, J_{HH} = 12.98 Hz, N–CH_2, aliphatic), 3.82 (s, 6H, 2×OCH_3), 3.49 (s, 1H, –NH), 1.43–1.29 (m, 8H, 4×CH_2, aliphatic), 0.96–0.84 (m, 6H, 2×CH_3, aliphatic). IR, (in Br), cm^{-1}: 3282 ν (NH); 3038, 2994 ν (CH_{ar}); 2953, 2926, 2836 ν ($CH_{aliphatic}$); 1688 ν (C=$O_{anhydride}$); 1647, 1575, 1503 ν (C=C_{ar}); 1462, 1440, 1427 γ (OCH_3); 1387, 1370, 1352 ν (C–N); 822, 775 γ (CH_{ar}); ^{13}C NMR spectrum (300 MHz, CDCl3, δ, ppm): 165.19, 164.70, 161.67, 156.82, 140.15, 134.42, 131.82, 131.70, 128.43, 128.32, 127.52, 125.60, 125.33, 123.53, 119.33, 116.98, 115.33, 115.13, 55.77, 44.23 38.24, 31.08, 29.04, 24.38, 23.36, 14.37, 10.96. MS (APCI$^+$, 20 V), *m*/*z*: 655 ([M + H]$^+$). Anal. Calcd. for $C_{41}H_{42}N_4O_4$: C, 75.20; H, 6.47; N, 8.56; O, 9.77. Found: C, 75.15; H, 6.42; N, 8.63; O, 9.84.

2.3.6. 4,4′-diformyl-4″-methoxyphenylamine bis(N-ethyl-N-(2-ethylhexyl)-1,8-naphthalimide) hydrazone (**5**)

Compound **3** (0.5 g, 0.51 mmol) and 30 ml of acetone were placed into a 100 ml 3-neck round bottom flask equipped with reflux condenser, thermometer and mechanical stirrer. The mixture was stirred vigorously at 50–60 °C for 10 min, during which of powdered potassium hydroxide KOH (0.072 g, 1.29 mmol), 1-iodoethane (0.094 g, 1.18 mmol) and tetrabutylammonium bromide (0.01 g, 0.032 mmol) were added. After 30 min the reaction mixture was filtered, and the solvent was evaporated. The crude product was purified by silica gel column chromatography using the mixture of acetone and *n*-hexane (vol. ratio 1:3) as an eluent. Yield: 0.38 g (53%) of red crystals. Mp = 94–95 °C ^{1}H NMR spectrum (300 MHz, CDCl3, δ, ppm): 8.67–8.58 (m, 5H, $H_{Naphthalene}$), 7.72 (dd, 3H, J_{HH} = 7.33 Hz, J_{HH} = 8.53 Hz, $H_{Naphthalene}$), 7.65 (s, 2H, $H_{Naphthalene}$), 7.53 (dd, 6H, J_{HH} = 2.34 Hz, J_{HH} = 8.48 Hz, ar), 7.13–7.07 (m, 4H, ar), 6.92–6.88 (m, 2H, ar), 4.18–4.16 (m, 4H, 2×N–CH_2, aliphatic), 3.85 (s, 3H, –OCH_3), 2.04–1.95 (m, 2H, 2×CH, alihatic), 1.46–1.36 (m, 20H, 10×CH_2, aliphatic), 1.13–0.74 (m, 18H, 6×CH_3, aliphatic). IR, (in Br), cm^{-1}: 3063 ν (CH_{ar}); 2955, 2926, 2856 ν ($CH_{aliphatic}$); 1691 ν (C=$O_{anhydride}$); 1696, 1656, 1585, 1505 ν (C=C_{ar}); 1465, 1426 γ (–OCH_3); 1386, 1352 ν (C–N); 828, 779 γ (CH_{ar}); ^{13}C NMR spectrum (300 MHz, CDCl3, δ, ppm): 165.08, 164.54, 150.96, 148.32, 139.97, 137.74, 132.22, 131.76, 131.65, 130.23, 129.74, 128.01, 127.54, 127.44, 126.19, 119.68, 118.40, 115.20, 55.76, 47.06, 44.35, 38.21, 31.04, 29.01, 24.34, 23.37, 14.39, 11.25, 10.96. MS (APCI$^+$, 20 V), *m*/*z*: 1030 ([M + H]$^+$). Anal. Calcd. for $C_{65}H_{71}N_7O_5$: C, 75.77; H, 6.95; N, 9.52; O, 7.76. Found: C, 75.68; H, 6.88; N, 9.59; O, 7.71.

2.3.7. 4-(Di(4-methoxyphenyl)amine)benzaldehyde N-ethyl-N-(2-ethylhexyl)-1,8-naphthalimide hydrazone (**6**)

Compound **6** was synthesized by the same procedure as compound **5**, only compound **4** was used instead of compound **3**. The yield of red crystals was 0.2 g (80%). Mp = 67–68 °C ^{1}H NMR spectrum (300 MHz, CDCl3, δ, ppm): 7.71 (d, 2H, J_{HH} = 1.25 Hz, $H_{Naphthalene}$), 7.68 (d, 1H, J_{HH} = 4.13 Hz, $H_{Naphthalene}$), 7.53 (s, 1H, $H_{Naphthalene}$), 7.49 (d, 1H, J_{HH} = 4.13 Hz, $H_{Naphthalene}$), 7.16–7.07 (m, 4H, ar), 7.02–6.81 (m, 8H, ar), 4.18–4.13 (m, 2H, N–CH_2, aliphatic), 3.83 (s, 6H, 2×OCH_3), 2.02–1.94 (m, 1H, N–CH, aliphatic), 1.47–1.33 (m, 10H, 5×CH_2, aliphatic), 1.01–0.86 (m, 9H, 3×CH_3, aliphatic). IR, (in Br), cm^{-1}: 3037 ν (CH_{ar}); 2954, 2927, 2856 ν ($CH_{aliphatic}$); 1695 ν (C=$O_{anhydride}$); 1655, 1585, 1504 ν (C=C_{ar}); 1464, 1441, 1427 γ (OCH_3); 1400 1385, 1353 ν (C–N); 826, 779 γ (CH_{ar}); ^{13}C NMR spectrum (300 MHz, CDCl3, δ, ppm): 165.17, 164.57, 156.44, 151.31, 149.69, 140.66, 138.80, 132.25, 131.94, 131.59, 127.55, 127.42, 127.15, 126.01, 120.12, 119.24, 118.04, 115.02, 55.77, 44.23 38.24, 31.08, 29.04, 24.38, 23.36, 14.37, 10.96. MS (APCI$^+$, 20 V), *m*/*z*: 683 ([M + H]$^+$). Anal. Calcd. for $C_{43}H_{46}N_4O_4$: C, 75.63; H, 6.79; N, 8.20; O, 9.37. Found: C, 75.58 H, 6.83; N, 8.15; O, 9.32.

3. Results and discussion

Compounds **3** and **4** containing electron-withdrawing naphthalimide moiety and electron-donating triphenylamino moiety were synthesized by the synthetic route, shown in Scheme 1. The first step was condensation of 4-bromo-1,8-naphtalic anhydride with 2-ethylhexylamine in DMF to obtain 4-bromo-*N*-(2-ethylhexyl)-1,8-naphthalimide (**1**). Compound **1** was treated with hydrazine hydrate to yield 4-hydrazino-*N*-(2-ethylhexyl)-1,8-naphthalimide (**2**). Compounds **3** and **4** were obtained by condensation of compound **2** with an excess of 4-(di(4-methoxyphenyl)amine)benzaldehyde (**a**) and 4,4′-diformyl-4″-methoxyphenylamine (**b**).

Compounds **5** and **6** were synthesized by alkylation of **3** and **4** in the presence of potassium hydroxide (Scheme 2).

The chemical structures of the newly synthesized compounds (**1**–**6**) were confirmed by ^{1}H NMR, ^{13}C NMR, IR, and mass spectrometries. Hydrazones **3**–**6** are soluble in common organic solvents such as chloroform, acetone, tetrahydrofuran (THF).

The behaviour under heating of compounds **3**–**6** was studied by DSC and TGA under a nitrogen atmosphere. The values of glass transition temperatures (T_g) and the temperatures of the onset of the thermal decomposition (T_{dec}) are summarized in Table 1.

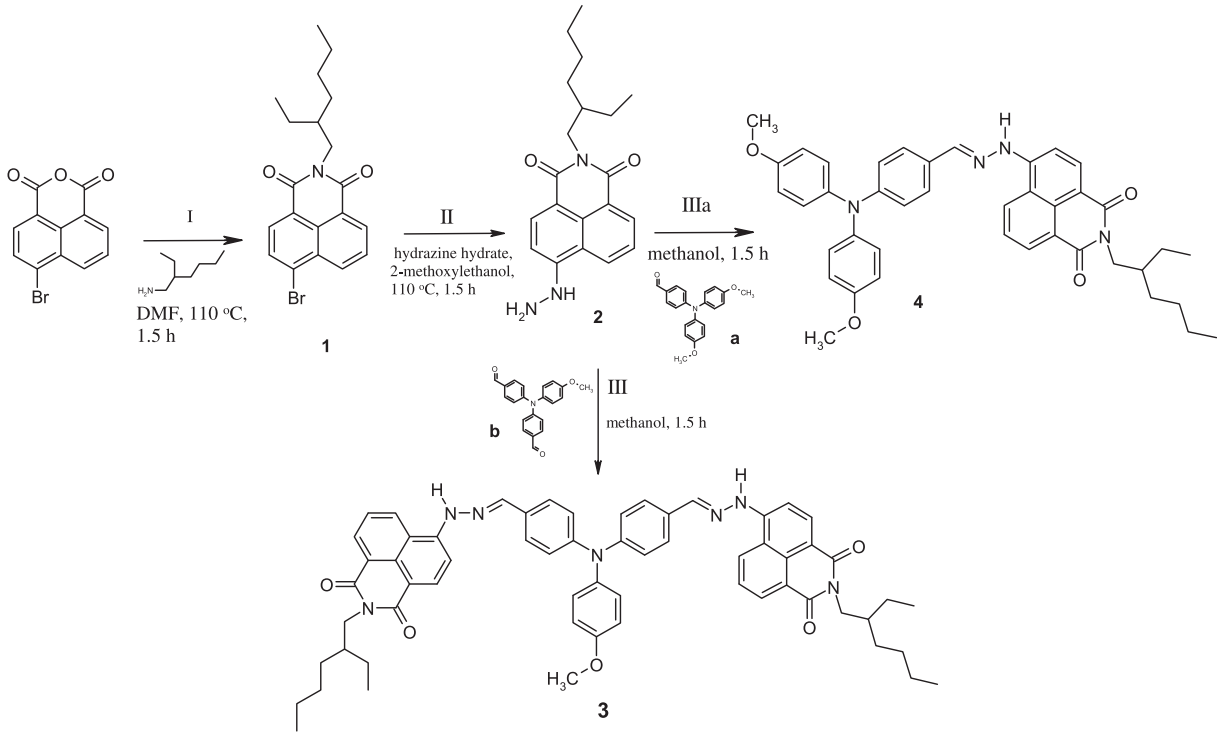

Scheme 1. Synthetic routes to hydrazones **3** and **4**.

Compounds **3**–**6** demonstrate thermal stability similar to that of other hydrazones [23]. The mass loss starts at the temperatures ranging from 268 °C to 348 °C as confirmed by TGA with a heating rate of 10 °C/min. Alkyl-substituted derivatives **5** and **6** exhibit lower thermal stability than the corresponding unsubstituted compounds (**3** and **4**). The attachment of ethyl group at the nitrogen atom of hydrazine moiety leads to the change of the mechanism of thermal degradation. While the degradation of unsubstituted compounds (**3** and **4**) occurs in one stage, the alkyl-substituted derivatives (**5** and **6**) show two-step thermal degradation. The thermal degradation of compounds containing hydrazine moiety usually starts from decomposition of this fragment [23]. Lower thermal stability of derivatives **5** and **6** having alkyl substituents at hydrazine moeities with respect of unsubstituted compounds (**3** and **4**) show that the thermal degradation of 5 and 6 starts by loosing the alkyl groups of hydrazine moieties. The examples of TGA curves are given in Supporting information.

The compounds synthesized can exist in the glassy state. Their glass transition temperatures range from 46 to 142 °C. The comparison of the glass transition temperatures of compounds **3** and **4** having secondary amino group with those of alkyl-substituted hydrazones **5** and **6** reveal considerably higher glass transition temperatures of **3** and **4**. This observation can apparently be explained by the hydrogen bonding in the glasses of **3** and **4**.

Fig. 1 show UV and fluorescence spectra of dilute solutions and of compounds **3**–**6**. The wavelengths of absorption and emission maxima are summarized in Table 2.

The absorption spectra of compounds **3**, **4** and **5**, **6** are similar. The lowest energy absorption bands of monohydrazones **4** and **6** are slightly red-shifted with respect of those of dihydrazones **3** and **5**. This observation can apparently be explained by the presence of two methoxy groups in triphenylamino moieties of monohydrazones The fluorescence spectra of compounds **3** and **4** are also similar. The spectrum of monohydrazone **4** shows bathochromic shift with respect of the spectrum of dihydrazone **3**. This observation is consistent with the UV spectrometry data. Fluorescence quantum yields of dilute THF solutions of **3** and **4** are 0.23 and 0.08 repectively. We did not observe fluorescence of **5** and **6** from dilute THF solutions however we did observe the emission of these compounds from dilute solutions in toluene (Fig. 1, Table 2).

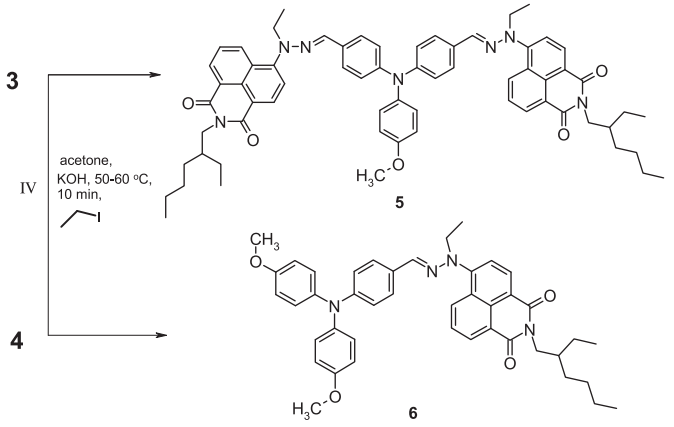

Scheme 2. Synthesis of compounds **5** and **6**.

Table 1
Temperatures of the thermal transitions of compounds **3**–**6**.

Compound	T_g [°C][a]	T_{dec} [°C]
3	142	275
4	87	348
5	73	268
6	46	303

[a] Glass transition temperature (T_g) was estimated from the second DSC heating scan.

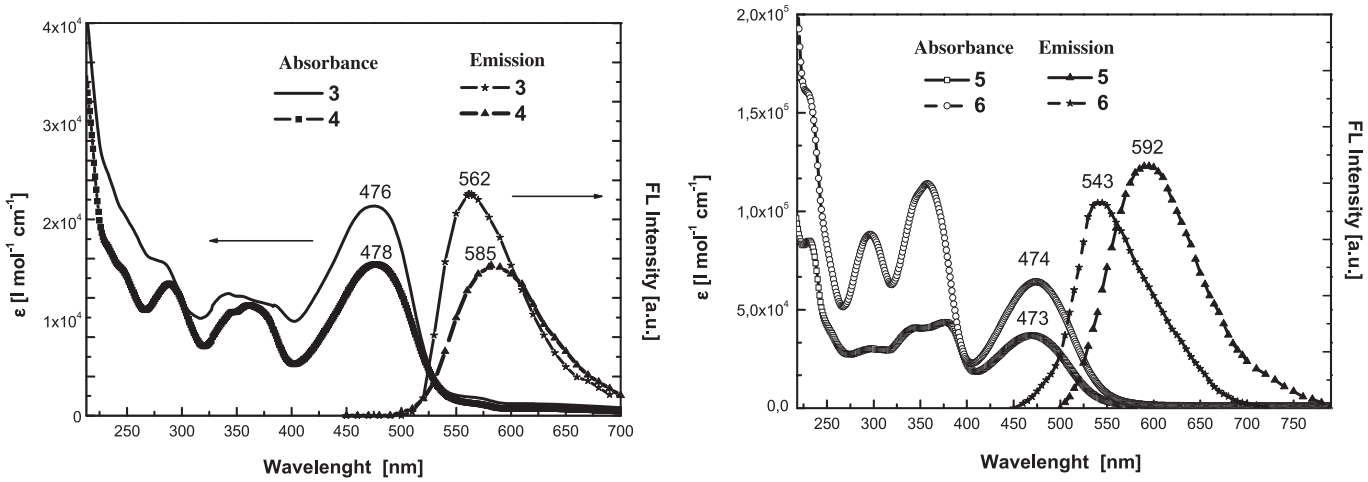

Fig. 1. UV–vis spectra of dilute THF solutions (10^{-5} M) of hydrazones **4**–**6**; FL spectra of **3**, **4** in THF solutions (10^{-5} M, $\lambda_{ex} = 310$ nm); FL spectra of **5**, **6** in toluene solutions (10^{-5} M, $\lambda_{ex} = 310$ nm).

Table 2
Wavelengths of absorption and fluorescence maxima of compounds **3**–**6**.

Compound	UV: λ_{max} [nm][a]	UV: λ_{max} [nm][b]	FL: λ_{max} [nm][a]	FL: λ_{max} [nm][c]
3	476	499	562	527
4	478	511	585	543
5	473	485	N.d	592
6	474	491	N.d	543

N.d – fluorescence not detectable.
[a] Solution in THF with the concentration of 10^{-5} M; for FL $\lambda_{ex} = 310$ nm.
[b] Measured as thin films onto fused quartz plates.
[c] Solution in toluene with the concentration of 10^{-5} M; $\lambda_{ex} = 310$ nm.

However these compounds seem to be photochemically unstable. The repeated recording of the fluorescence spectra of the solutions of these compounds gives decreased intensity. Red shifts of fluorescence spectra of THF solutions of **3**, **4** relative to those of toluene solutions of the same compounds (Table 2) can be explained by higher dipole moment of THF, which results in the enhanced Stokes shifts.

Absorbtion spectra of the films of compounds **3**–**6** (Fig. 2) are similar to those of dilute solutions, however the lowest energy absorption bands of the films are red-shifted with respect of those of the solutions, apparently due to enhanced intermolecular interactions in the solid state. Bathochromic shifts of the spectra of the films with respect of the spectra of solutions are more evident for compounds **3** and **4** relative to compounds **5** and **6**. The intermolecular interaction in the films of unsubstituted hydrazones is apparently stronger due to hydrogen bonding. We did not manage to record fluorescence from the films of compounds **3**–**6**. This was apparently due to the intermolecular quenching.

Electrochemical investigation of dichloromethane solutions of compounds showed that oxidation starts at the same potential of 0.09 V as shown in Fig. 3a–d. The first oxidation potential of compounds occurs at 0.30 V for **3** and at 0.25 V for **4**. Oxidation of **3** and **4** is a reversible redox process but the reduction process is reversible only for **5** and **6** (Fig. 3a,c). The first reduction potential occured at −1.86 V, −1.84 V for compounds with alkyl chain (**5**, **6**) and at −1.97 V, −1.99 V for compounds with unsubstituted hydrazine moiety (**3**, **4**).

CV curves of monohydrazones **4**, **6** are shifted negatively as compared to the curves of dihydrazones **3**, **5**. The shapes of CV curves are similar for alkyl-substituted compounds **5** and **6** (cf.

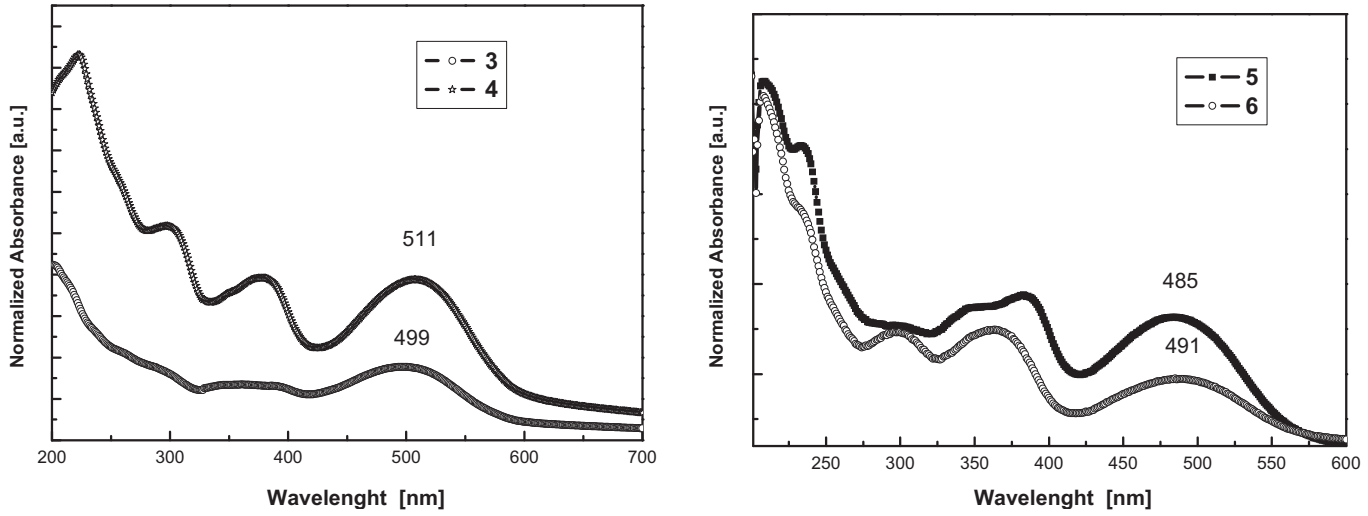

Fig. 2. UV–vis absorption spectra of thin films of hydrazones **3**–**6**.

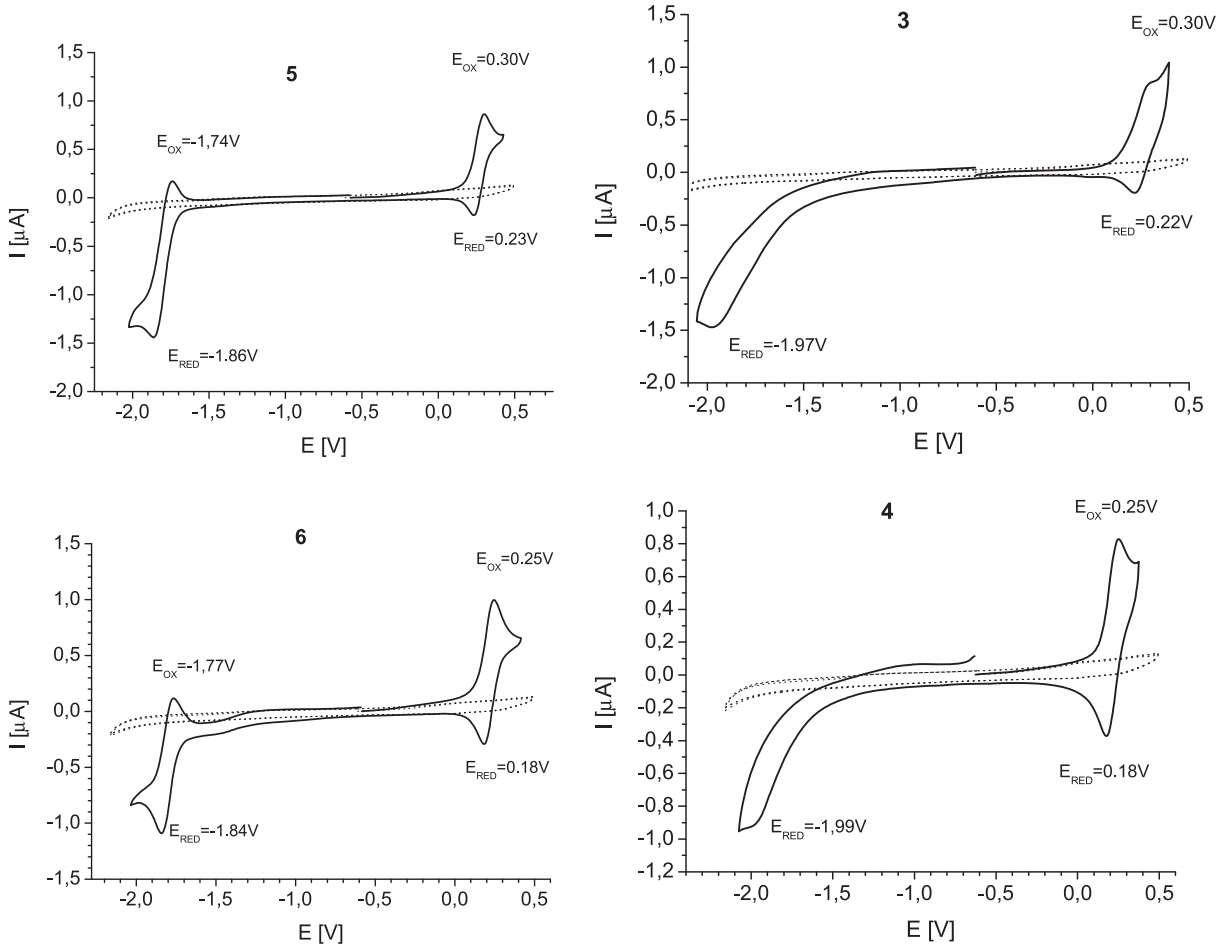

Fig. 3. Cyclovoltammperometric (CV) curves of 1 mM solutions in 1 M Bu_4NBF_4 dichloromethane electrolyte of a) **5**; b) **3**; c) **6**; d) **4**. Measurement conditions: scan rate 50 mV/s, Ag wire – calibrated versus ferrocene/ferrocinium redox couple as a quasi-reference electrode.

curves Fig. 3a,c) They are also similar for unsubstituted derivatives (**3** and **4**) (cf. curves Fig. 3b,d). However the considerable distinctions are observed between CV curves of alkyl-substituted (**5**, **6**) and unsubstituted (**3**, **4**) compounds (cf. curves Fig. 3a,b). Free hydrogen at hydrazine nitrogen is apparently involved in side reactions of electrochemical process and because of that reduction process is not reversible. Oxidation part of CV curves is related to the oxidation of triphenylamino group and reduction part is related to the reduction of imido group.

DPV spectra (Fig. 4) show absolute peaks of oxidation and reduction processes. In correlation to the molecular band, oxidation peak is related to the HOMO band and reduction peak is related to the LUMO band. Electrochemical band-gap value is the range between those peaks. Oxidation potential peaks are similar for monohydrazones **4** and **6** (0.21 V) and dihydrazones **3** and **5** (0.16 V). For reduction potential peaks opposite correlation is observed: potential is similar for compounds with alkyl group **5**, **6** (−1.80 V) or without it **3, 4** (−1.89 V).

The band-gap value is one of the most useful characteristic for materials used in optoelectronic devices. Electrochemical band gap is usually slightly lower than the optical one. The band-gap values for the alkyl-substituted hydrazones **5**, **6** are lower than those of unsubstituted hydrazones **3** and **4**. Alkyl-substituted hydrazones **5**,**6** show lower energy of LUMO band than their unsubstituted counterparts. Compounds 4 and 6 having two methoxy groups in triphenylamino moiety show increased energy of HOMO band (see Table 3).

The E_{HOMO} values determined by cyclic voltammetry do not represent any absolute solid-state or gas-phase ionization energies, they can be used only for the comparison of different compounds. It was therefore of interest to estimate the ionization potentials of the

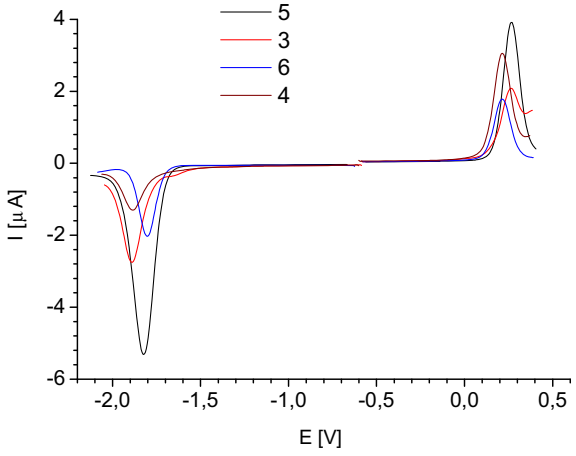

Fig. 4. Differential pulse voltammperometric (DPV) curves of 1 mM of compounds **3**–**6** in 1 M Bu_4NBF_4 dichloromethane electrolyte. Measurement conditions: scan rate 50 mV/s, Ag wire – calibrated versus ferrocene/ferrocinium redox couple as a quasi-reference electrode.

Table 3
HOMO–LUMO energy levels, optical and electrochemical band-gap energies and ionization potentials of bipolar hydrazones.

Copmound	E_{HOMO} [eV]	E_{LUMO} [eV]	E_G [eV] electr.	E_G [eV] opt.	I_p [eV][a]
3	−5.06	−2.91	2.15	2.27	–
4	−5.01	−2.91	2.10	2.27	–
5	−5.06	−3.00	2.06	2.24	5.45
6	−5.01	−3.00	2.01	2.25	5.45

[a] Established from electron photoemission in air spectra.

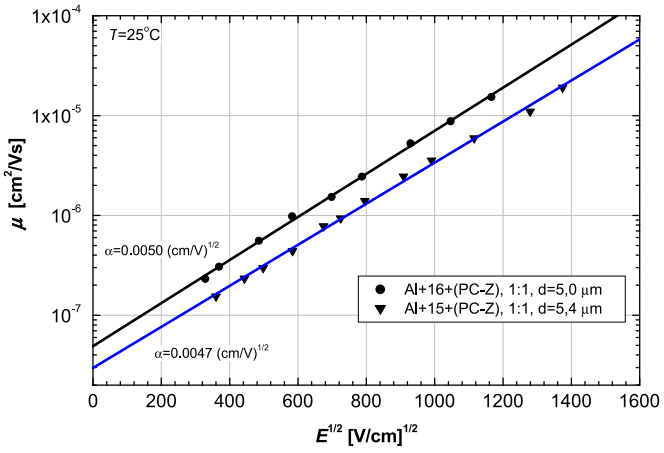

Fig. 5. Electric field dependencies of hole-drift mobilities in the layers of hydrazones **5** and **6** molecularly doped in PC-Z (50 wt.%).

amorphous layers of the synthesized compounds. The values of ionization potentials of compounds **5** and **6** are given in Table 3. It seems that the presence of electron-accepting 1,8-naphthalimide species has minor effect on the ionization potentials of these compounds. They are close to the ionization potentials of earlier reported triphenylamine-based hydrazones [24,25].

Xerographic time-of-flight measurements were used to characterize the magnitudes of hole-drift mobility (μ_h) for the solid solutions of compounds **5** and **6** in the host polymer bisphenol-Z polycarbonate (PC-Z). For the layers of compounds **5** and **6** in PC-Z the room temperature μ_h shows the linear dependencies on the square root of the electric field (Fig. 5). This characteristic dependence is observed for the majority of amorphous organic systems and can be attributed to the effects of disorder on charge transport [26]. The layers of the solid solutions of compounds **5** and **6** in PC-Z (50%) showed μ_h exceeding 10^{-5} cm^2 V^{-1} s^{-1} at high electric fields at 25 °C.

4. Conclusions

Four new hydrazones containing both acceptor and donor moieties were synthesized and their thermal, optical, electrochemical and photoelectrical properties were investigated. The HOMO–LUMO energy levels, optical and electrochemical band-gap energies and ionization potentials were established. The hydrazones exhibit initial mass loss temperatures in the range of 268–348 °C and can form glasses with glass transition temperatures in the range of 46–142 °C. Room temperature time-of-flight hole mobilities in the solid solutions of the derivatives in the polymeric host bisphenol-Z polycarbonate (50%) exceeded 10^{-5} cm^2/V s at high applied electric fields. The ionization potentials of the alkyl-substituted compounds, measured by electron photoemission technique are 5.45 eV.

Acknowledgements

Financial support by the Research Council of Lithuania (project No MIP-64/2010) is gratefully acknowledged. Habil. Dr. V. Gaidelis from the Department of Solid State electronics, Vilnius University is thanked for the help in the measurements of ionization potentials.

Appendix. Supporting information

Supporting information related to this article can be found at doi:10.1016/j.dyepig.2011.02.002.

References

[1] Sun YD, Duan L, Wei P, Qiao J, Dong GF, Wang LD, Qiu Y. Org Lett 2009;11:2069.
[2] Takizawa SY, Montes VA, Anzenbacher P. Chem Mater 2009;l21:2452.
[3] Tsuji H, Mitsui C, Sato Y, Nakamura E. Adv Mater 2009;21:1.
[4] Wu H, Zou J, Liu F, Wang L, Mikhailovsky A, Bazan GC, et al. Adv Mater 2008;20:696.
[5] Chien CH, Shih PI, Wu FI, Shu CF, Chi YJ. Polym Sci Part A: Polym Chem 2007;45:2073.
[6] Grimsdale AC, Chan KL, Martin RE, Jokisz PG, Holmes AB. Chem Rev 2009;109:897.
[7] Burgi L, Turbiez M, Pfeiffer R, Bienewald F, Kirner HJ, Winnewisser C. Adv Mater 2008;20:2217.
[8] Ning ZJ, Tian H. Chem Commun 2009;37:5483.
[9] Leng B, Tian He. Austr J Chem 2010;63:169.
[10] Wang S, Zeng PJ, Liu YQ, Yu G, Sun XB, Niu HB, et al. Synth Met 2005;150:33.
[11] (a) Zhu WH, Hu M, Wu YQ, Tian H, Sun RG, Epstein AJ. Synth Met 2001;119:547;
(b) Tian H, Su JH, Chen KC, Wong TC, Gao ZQ, Lee CS, et al. Opt Mater 2000;14:91;
(c) Jiang X, Liu Y, Tian H, Qiu W, Song X, Zhu D. J Mater Chem 1997;7:1395;
(d) Cacialli F, Friend RH, Bouche CM, Le Barny P, Facoetti H, Soyer F, et al. J Appl Phys 1998;83:2343.
[12] (a) Strohriegl P, Grazulevicius JV. Adv Mater 2002;14:1439;
(b) Van Slyke SA, Tang CW. US patent no. 1985;507:4539.
[13] Lo S-C, Burn PL. Chem Rev 2007;107:1097.
[14] Shirota Y, Kageyama H. Chem Rev 2007;107:953.
[15] Hua JL, Li B, Meng FS, Ding F, Qian SX, Tian H. Polymer 2004;45:7143.
[16] Harwood LM, Moody CJ. Organic chemistry. Principles and practice. Blackwell Science; 1989.
[17] Montrimas E, Gaidelis V, Pazera A. Lithuanian J Phys 1966;6:578.
[18] Vaezi-Nejad SM, Int J. Electronics 1987;62:361.
[19] Grigalevicius S, Getautis V, Grazulevicius JV, Gaidelis V, Jankauskas V, Montrimas E. Mater Chem Phys 2001;72:395.
[20] Kirkus M, Tsai M-H, Grazulevicius JV, Wu C-C, Chi L-C, Wong K-T. Synth Met 2009;159:729.
[21] Vilsmeier V, Haack A. Berichte Dtsch Chem Ges 1927;60:119.
[22] Gan J, Tian H, Wang Z, Chen K, Hill J, Lane PA, et al. J Organomet Chem 2002;645:168.
[23] Ostrauskaite J, Voska V, Grazulevicius JV. Monatsh Chem 2002;133:599.
[24] Getautis V, Grazulevicius JV, Daskevicienė M, Malinauskas T, Jankunaite D, Gaidelis V, et al. Polymer 2005;46:7918–22.
[25] Lygaitis R, Getautis V, Gražulevičius JV. Chem Soc Rev 2008;37:770–88.
[26] Borsenberger M, Weiss DS. Photoreceptors for imaging systems. New York: Marcel Dekker; 1993.